communications physics

ARTICLE

https://doi.org/10.1038/s42005-022-00955-7 OPEN

Universal stripe order as a precursor of the superconducting phase in pressurized $BaFe_2Se_3$ Spin Ladder

Wen-Gen Zheng[1], Victor Balédent[1], Claire V. Colin[2], Françoise Damay[3], Jean-Pascal Rueff[4,5], Anne Forget[6], Dorothée Colson[6] & Pascale Foury-Leylekian[1✉]

It has been recently observed that a superconducting phase emerges under pressure in the Fe-based spin-ladders $BaFe_2X_3$ (X = S, Se). The low dimensionality of the Fe spin-ladders, which simplifies the elaboration of theoretical models, should help to understand the mechanism of superconductivity. We investigate here the frontier between magnetic and superconducting (SC) phases in $BaFe_2Se_3$ by performing challenging powder neutron diffraction (PND) and Fe K_β x-ray emission spectroscopy (XES) under high pressure. We show that the ambient pressure ground state with a block-like magnetic order is destabilized under pressure. A pressure-induced antiferromagnetic stripe-like spin order, similar to the magnetic order of the parent superconductor $BaFe_2S_3$, is observed above 3-4 GPa. Our discovery shows that the stripe magnetic order is a key phase close to the SC dome and its particular magnetic fluctuations could be involved in the stabilization of superconductivity in Fe-based spin ladders.

[1] Université Paris-Saclay, CNRS, Laboratoire de Physique des Solides, 91405 Orsay cedex, France. [2] Institut Néel, Université Grenoble Alpes, CNRS, Grenoble F-38042, France. [3] Laboratoire Léon Brillouin, CEA-CNRS UMR12, 91191 Gif-sur-Yvette Cedex, France. [4] Synchrotron SOLEIL, L'Orme des Merisiers, BP 48 St Aubin, 91192 Gif-sur-Yvette, France. [5] Laboratoire de Chimie Physique-Matière et Rayonnement, Sorbonne Université, CNRS, 75005 Paris, France. [6] SPEC, CEA, CNRS-UMR3680, Université Paris-Saclay, Gif-sur-Yvette Cedex 91191, France. ✉email: pascale.foury@universite-paris-saclay.fr

Unconventional superconductivity and magnetism seem to be mutually exclusive in most cases. However, magnetic order is a necessary foe of unconventional superconductivity: it is systematically present in the vicinity of the superconducting phase. Furthermore, it is generally accepted that the presence of fluctuations associated with this magnetic phase contributes to the pairing of Cooper pairs in some SC systems. This is the case in the large families of heavy fermions[1,2], organic compounds[3], iron-based pnictides[4,5], or high critical temperature cuprates[6]. Thus the description and understanding of these neighboring magnetic phases are considered as an essential step to discovering a new pairing mechanism. However, a difficulty is encountered in modeling these mostly two-dimensional compounds. Besides, the range of theoretical tools, more precise or even exact, is much wider for one-dimensional systems[7]. Therefore, seeking one-dimensional superconducting compounds becomes essential for studying unconventional superconductivity.

To the best of our knowledge, $BaFe_2X_3$ (X = S and Se) are the first quasi-one-dimensional iron-based superconductors without a square-lattice motif[8,9]. They are composed of two iron ladders per unit cell. The average structure of $BaFe_2Se_3$ has the *Pnma* symmetry, while $BaFe_2S_3$ crystallizes in the *Cmcm* space group[10], as described in Fig. 1a, b. The FeX_4 tetrahedra are aligned in the horizontal plane for the *Cmcm* structure while exhibiting a tilt in *Pnma*. Importantly, we recently solved the exact structure of $BaFe_2Se_3$ which is polar with a $Pmn2_1$ space group[11]. This symmetry allows a possible ferroelectric character already at room temperature, as previously proposed by ref. [12]. However, it is impossible to distinguish between both space groups from powder diffraction data under pressure. In addition, the very weak structural differences between $Pmn2_1$ and *Pnma* have no influence on the magnetic structure. Therefore, in the following, we will use the notation $Pmn2_1$/*Pnma* to describe the ambient pressure and high-temperature symmetry. Moreover, to avoid confusion in the rest of the paper, we will use the directions of the *Pnma* setting even for the *Cmcm* structure when we describe the direction of the Fe spins.

In $BaFe_2S_3$, a stripe-like magnetic structure with a propagation wave vector $\vec{k} = \frac{1}{2}, 0, \frac{1}{2}$ is stabilized below $T_N = 119$ K with the moments of Fe along the *c*-axis[8]. The superconductivity appears at about 11 GPa with the suppression of the stripe magnetic order[8]. For $BaFe_2Se_3$ an unusual block-like Néel order establishes below $T_N = 140-250$ K with a reduced propagation wave vector $\vec{k} = \frac{1}{2}, \frac{1}{2}, \frac{1}{2}$ (Fig. 1c). The large range of T_N values[13–17], originates from slight deviations to the ideal $BaFe_2Se_3$ stoichiometry[18–20]. In $BaFe_2Se_3$, the magnetic order is characterized by the antiferromagnetic (AFM) arrangement along the ladder of square-like blocks containing four ferromagnetically ordered Fe spins (Fig. 1c)[21]. Previous powder neutron diffraction experiments[13,15,21] found that the Fe spins are mostly parallel to the *a*-axis. Along the leg of the ladders, the up–up–down–down spin motif is the fingerprint of a magnetic frustration issued from competing exchange interactions present in this system[17]. Interestingly, the ordered magnetic moments on the Fe sites are small, even at low temperature ($2.8\mu_B$)[13], compared to the theoretical moment expected for a high spin Fe^{2+} moment ($4\mu_B$). This can be attributed to the coexistence of the itinerant and Mott localized electrons due to an orbital selective Mott phase[13,15]. As for the magnetic structure under pressure, close to the superconducting phase, it remains unknown even though it constitutes a necessary starting point, from which the superconductivity under pressure emerges.

In this context, numerous investigations and predictions have been proposed for $BaFe_2Se_3$[9,12,22–26], in particular under pressure[9,19,27–29]. It has been shown that a second-order phase transition from $Pmn2_1$/*Pnma* to *Cmcm* space group occurs between 4 and 6 GPa, depending on the pressure transmitting medium (PTM) used[19,27]. At this pressure, the ratio *a*/*c* between the unit cell parameters reaches a value (1.28) very close to the one (1.277) of $BaFe_2S_3$ at ambient pressure in the *Cmcm* structure, which confirms that changing S by a larger Se atom acts as negative pressure. Recently, resistivity and susceptibility measurements, as well as Fe K_β XES under pressure, evidenced that the system is a Mott-insulator at ambient pressure[9]. A metal–insulator transition occurs at about 7.5 GPa followed by a SC state above 10 GPa[9]. The SC dome extends from 10 to 15 GPa with a maximum of $T_c = 11$ K at 12.5 GPa. Concomitantly, the local Fe moment measured by XES at the Fe edge decreases upon pressure[9]. It is noteworthy that in the SC phase, while the Néel

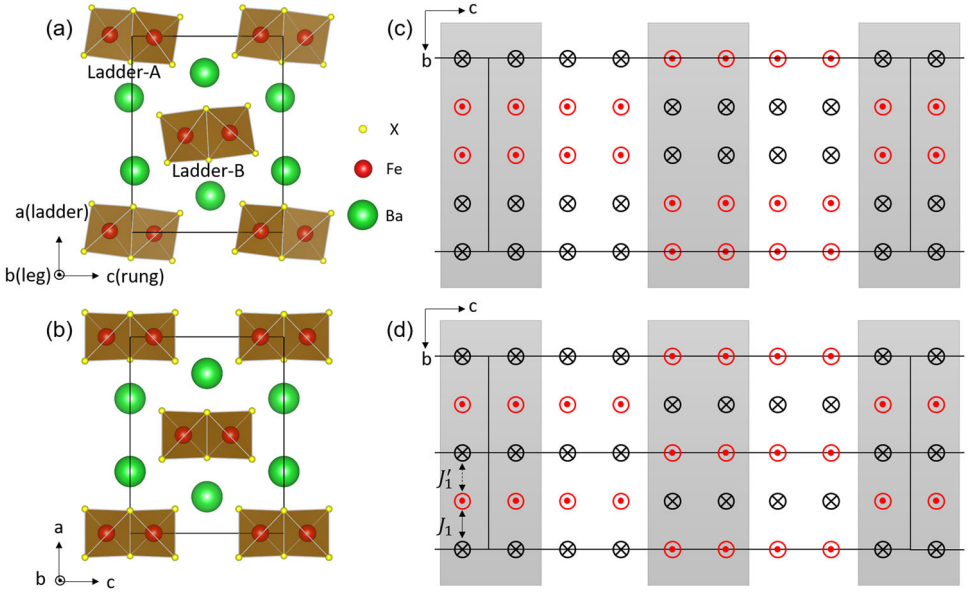

Fig. 1 Crystal and magnetic structures of $BaFe_2X_3$ (X = Se,S). a and **b** Atomic structures of $BaFe_2X_3$ viewed along *b*-axis in *Pnma* and *Cmcm* space groups, respectively. There are two ladders (Ladder-A and Ladder-B) in each unit cell. **c** and **d** Projections of Fe spins on the *bc*-planes of the Block and CX magnetic orders. The moments are perpendicular to the *bc* plane. The black lines indicate the edges of the magnetic unit cell. The two Fe ladders are separated by different background colors, gray for Ladder-A and white for Ladder-B.

order is suppressed, the Fe local moment remains finite and equal to $1\mu_B$ (±0.3)[9].

In addition, a systematic investigation of the physical properties of $BaFe_2Se_3$ by DFT calculations under pressure has been reported[28]. This work confirms that the structure smoothly transforms from $Pmn2_1/Pnma$ to $Cmcm$ at around 6 GPa. It also proposes that the system becomes metallic at 10.4 GPa and the unique ambient-pressure block antiferromagnetic ground state is replaced by the more common stripe AFM order (called CX) at 12 GPa which settles in the middle of the SC dome. The CX magnetic order is shown in Fig. 1d. So far, these interesting theoretical results have not been validated experimentally probably because of the challenge of high-pressure measurements. Very recently, a first neutron scattering experiment under pressure has been performed up to 6.8(3) GPa and 120 K[29]. Due to technical difficulties, the measurements have not been done in the SC phase, but the authors conclude that $BaFe_2Se_3$ displays a persistent block magnetism across a wide pressure range. However, above 3.7 GPa, T_N is strongly reduced as well as the ordered moment, and only a short-range magnetic order remains above 5.5 GPa.

For $BaFe_2Se_3$, a clear description of the magnetic state close to the SC phase and in the SC dome is still missing. The competition between the block magnetic state and other possible magnetic orders, such as the stripe-like one, should be considered. To investigate this issue, we performed the powder neutron diffraction and Fe K_β XES measurements under high pressure, particularly in the SC dome. We show that the block magnetic order is unstable toward a stripe-like CX magnetic structure above 3 GPa, not detected in reference[29]. This structure persists at higher pressure up to 7.7 GPa. In the SC phase, the disappearance of the magnetic phase was observed even if it is difficult to assess perfectly due to a decreasing signal-to-noise ratio at high pressure. Our study establishes that the stripe magnetic order appears as a universal precursor of the pressure-induced SC phase in $BaFe_2S_3$ and $BaFe_2Se_3$.

Results

We first performed X-ray diffraction measurements under multiple pressures to investigate the structural transition from $Pmn2_1/Pnma$ to $Cmcm$. The details are shown in Supplementary Note 1. We found that our sample presents a $Cmcm$ symmetry already under 3.2 GPa. Thus, the $Cmcm$ space group was used for all the refinements above 3 GPa in our paper.

To check the magnetic structure at ambient pressure, powder neutron diffraction measurements were performed at various temperatures. The complete results are given in Supplementary Note 2. The measurement evidence the occurrence of a magnetic order below 208 K (±10) and characterized by a magnetic propagation wave vector of $\vec{k} = (\frac{1}{2}, \frac{1}{2}, \frac{1}{2})$. T_N was found slightly smaller than the one obtained in refs. [15,19,30]. We checked the stoichiometry of our compound by Energy Dispersive Spectroscopy (EDS) and by refining the occupancy parameters in the neutron diffractograms. From EDS we obtained a maximum deviation of the Fe content of 2% and a maximum Se deficiency of 10 % (depending on the position of the beam on the sample)[11]. From the refinement, we obtained for each element, occupancy rates close to the nominal ones within the uncertainties of 2–3%. Besides, a short-range magnetic order is observed up to 275 K similarly to references[15,30] (Supplementary Fig. 2b). The magnetic structure was refined using the Block model in Fig. 1c. The thermal evolution of the magnetic moment per Fe led to a critical exponent of 0.2 which is closer to an Ising model than a mean-field one. The moment saturated below 50 K at $2.5\mu_B$ (±0.1).

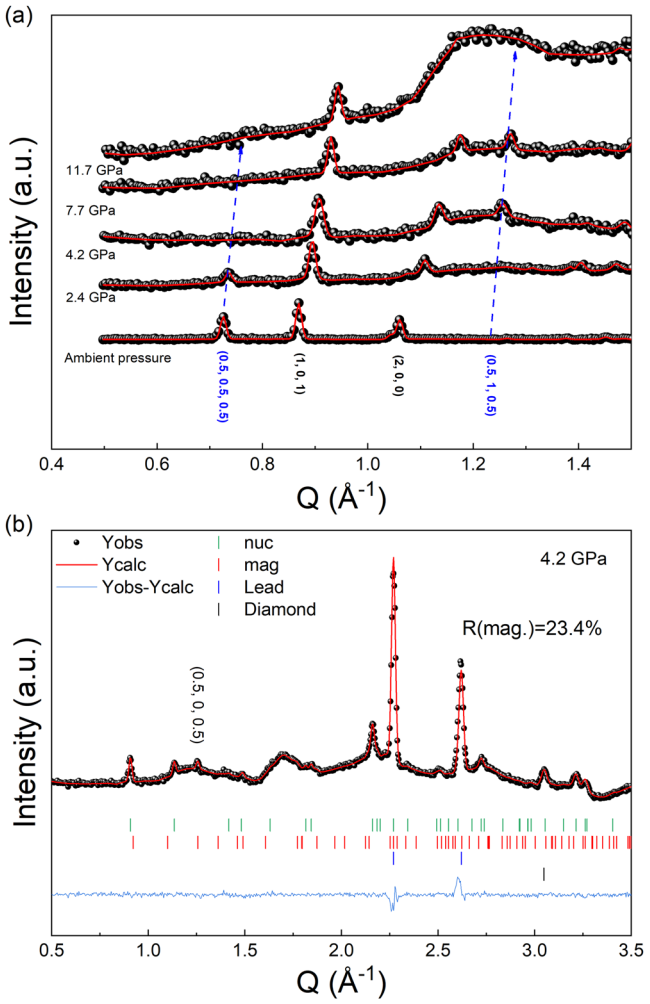

Fig. 2 Powder neutron diffraction patterns under pressure. a Evolution of the powder neutron diffraction (PND) patterns with increasing pressure. The magnetic reflection shifts to (0.5, 1, 0.5) when the pressure reaches 4.2 GPa. All patterns are measured at 3 K. To facilitate the comparison between different patterns, all the (1, 0, 1) reflections are put at the same scale. The blue arrow indicates the shift of magnetic reflections (0.5, 0.5, 0.5) ($Q \sim 0.73$ Å^{-1}) and (0.5, 1, 0.5) ($Q \sim 1.26$ Å^{-1}) when the pressure increases. The red lines are the fitted curves with the nuclear and magnetic phases obtained by Fullprof. **b** PND pattern of $BaFe_2Se_3$ at 3 K under 4.2 GPa. The red line indicates the fitted curve with the $Cmcm$ space group and CX magnetic order. The whole patterns for other pressures are shown in Supplementary Note 3.

The first high-pressure pattern was measured at 2.4 GPa (±0.41) and 3 K (the pressure given in the following are all measured at 3 K). We recorded a diffractogram for 10 h and detected the same $(\frac{1}{2}, \frac{1}{2}, \frac{1}{2})$ magnetic reflections as at ambient pressure (Fig. 2a). The adjustment of the calculated pattern with the data using the same block model leads to an ordered moment of $1.4\mu_B$ (±0.2). Since we have fewer magnetic reflections emerging from the background due to the pressure cell under pressure, the error bar for the moment amplitude is larger than that at ambient pressure. A Néel temperature of 110 K (±20) was determined by repeatedly measuring the diffractogram while the temperature was increased (for details see Supplementary Note 4). The decrease of both T_N and the ordered Fe moment at low temperature indicates that the block-like magnetic order is destabilized by the applied pressure above a critical pressure. This is not in agreement with the measurements of ref. [29], which

claimed that the ambient pressure magnetic structure is robust under intermediate pressures. An effect of sample dependence due to the slight Se deficiency of our sample can explain this discrepancy in the critical pressure.

At 4.2 GPa (±0.4), the background coming from the pressure cell starts to increase significantly due to the gasket crushing and the closure of its hole, which requires a longer acquisition time. Nevertheless, it was possible to determine that the nuclear phase adopts a *Cmcm* symmetry at this pressure. Figure 2b shows the refinement of the pattern with the *Cmcm* space group. In addition, we were able to observe a total loss of intensity on the $(\frac{1}{2},\frac{1}{2},\frac{1}{2})$ magnetic reflection concomitantly to the appearance of another magnetic reflection, indexed by $(\frac{1}{2},1,\frac{1}{2})$ as presented in Fig. 2a. This observation is the indication of a pressure-induced magnetic phase transition. This magnetic transition occurs at a pressure very close to the structural transition from $Pmn2_1$/*Pnma* to *Cmcm*. In order to investigate this high-pressure magnetic phase, we first determined its T_N. The long exposure times necessary at the high-pressure limit the number of diffractograms collected and prohibit the accurate determination of T_N. We obtained $T_N = 100$ K (±50) (Supplementary Note 4). Interestingly, this pressure-induced magnetic transition was not observed by the authors of ref. [29]. But their measurement was performed at 6 GPa and 120 K which is well above the critical pressure of 4.2 GPa but above T_N.

Concerning the magnetic order itself, it is important to remark that its propagation wave vector is incompatible with a block-like magnetic structure because the latter implies necessarily a doubling of the unit cell along the *b*-axis. To proceed with the analysis, we first tested various stripe-like models from ref. [28]. Except for the CX stripe-like magnetic model, none of them led to a correct fit of the data. The adjustment of the data with the CX model is shown in Fig. 2b. In this CX magnetic structure, each rung of the ladder is constituted of two Fe spins directed along *a*. The rungs are then AFM ordered along the *b*-axis (Fig. 1d). This magnetic order is similar to the ones stabilized in the analog systems $BaFe_2S_3$[8] and KFe_2S_3[30], except concerning the direction of the moments. In $BaFe_2Se_3$, at least at ambient pressure, a strong spin anisotropy aligns the moments along *a*[14,22]. A reorientation of the spins under pressure is however possible as the other compounds of the series present different axial anisotropies. We thus tried different CX stripe models with spins along *a*, *b* and *c* to adjust our data. The model with moments along *a* gave the best adjustment ($R_{mag} = 23.4\%$, $R_{mag.} = 71.61\%$, $R_{mag.} = 38.55\%$ for the spins along *a*, *b*, and *c* respectively) with an ordered magnetic moment on the Fe site of 2.1 μ_B (±0.2).

Under 7.7 GPa (±0.4), the results are found to be similar to that under 4.2 GPa and confirm the presence of a pressure-induced phase (Fig. 2a). The adjustment of the experimental data with the same CX model gives an ordered magnetic moment on the Fe of 1.9μ_B (±0.3). Interestingly, T_N at 7.7 GPa is between 110 and 150 K which is higher than that at 4.2 GPa (Supplementary Note 4). The same T_N behavior with increasing pressure in the stripe magnetic phase is also observed in $BaFe_2S_3$[31]. It is noteworthy that, at 7.7 GPa, the amplitude of the ordered moment at low temperature is comparable to the one at 4.2 GPa and thus that the CX magnetic order is robust under pressure. However, the ordered moment is considerably smaller than the one expected for a high spin configuration of the Fe^{2+} ions. This result can be explained either by the orbital selective Mott phase scenario or by the modification of the crystal field under pressure leading to $S = 1$, where *S* is the local moment of the Fe ion[32].

The last pattern was obtained under 11.7 GPa (±0.5) (Fig. 2a). At this pressure, no obvious magnetic reflection was detected within the error bars (±1μ_B) due to the strong background. So, given the accuracy of the measurement, if there is an ordered moment, its maximum amplitude is 1μ_B on the Fe ion.

We thus show here that the CX magnetic order, robust between 4.2 and 7.7 GPa, is destabilized above 7.7 GPa. Most interestingly, we evidence that the CX magnetic structure makes the border with the SC dome in the (*P*,*T*) phase diagram. This means that the superconductivity emerges from the CX phase. This is further supported by the fact that our experiment at 11.7 GPa cannot totally exclude the coexistence of a weak CX phase with the superconducting state.

In various systems, the magnetic atoms carry local moments which do not order or only partly order at low temperature. It is the case in frustrated magnets[33] and in orbital selective Mott phases[26]. Interestingly, in orbital selective Mott systems, the coexistence of an SC and a magnetic phase is not excluded. So local and ordered magnetic moments are two different parameters that are both important to measure. To probe the local magnetic moment on the Fe site, we performed XES at the Fe K_β emission line at the GALAXIES beamline of Synchrotron SOLEIL. The pressure was applied using a membrane-driven diamond-anvil cell (DAC) equipped with 1.7-mm-thick diamonds with 900 µm culets. $BaFe_2Se_3$ powder was loaded in a 300-µm hole of an Inox gasket, along with ruby chip for in situ pressure measurement and silicone oil as a pressure transmitting medium. We recorded the XES spectra as a function of pressure up to 14.7 GPa at room temperature (partially shown in Supplementary Note 5), knowing that the local moment of $BaFe_2Se_3$ does not change with temperature[9]. An integrated absolute difference (IAD) analysis was used to obtain the total local moment (*S*) on the Fe site by taking the FeS_2 spectrum as a reference of non-magnetic Fe ($S = 0$). The pressure dependence of S/S_0 is shown in Fig. 3 (right axis) where S_0 is the local moment at ambient pressure. We can see that in the $Pmn2_1$/*Pnma* phase (between 0 and 3 GPa), the local magnetic moment is roughly constant within the error bars. Above 3–4 GPa it undergoes a monotonous decrease up to 8 GPa. We evidence here the influence of the magnetic and structural transition on the local magnetic moment. Above 8 GPa, close to

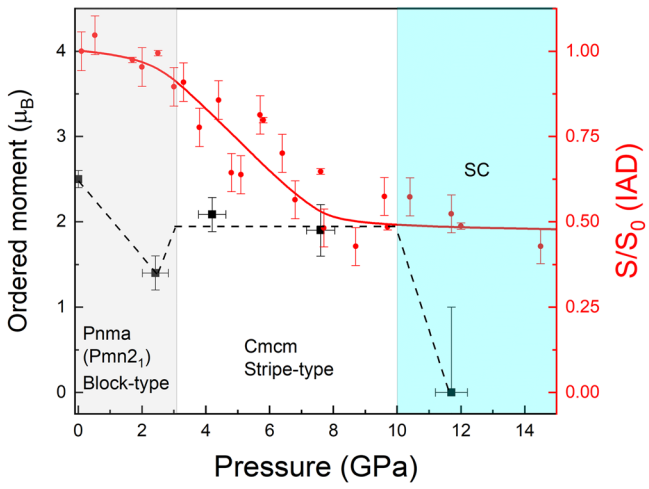

Fig. 3 Pressure dependence of ordered and local moments. Pressure dependence of ordered moment per Fe from powder neutron diffraction (PND) at 3 K (black squares, left scale). The error bars come from the uncertainty of the refinement. Local moment under pressure *S* versus local moment at ambient pressure S_0 (red circles, right scale) deduced from the x-ray emission spectroscopy (XES) by the integrated absolute difference (IAD) analysis at 300 K. The error bars are determined using the square root of the number of photons detected in the energy range 7042–7058 eV for each spectrum. The red solid and black dash lines are the guides for the eyes.

the SC border, the local moment roughly stabilizes at a non-zero value. The presence of a finite local moment in the SC dome has also been observed in reference[9] showing in addition that the local moment only disappears above 30 GPa.

The pressure dependence of ordered moment extracted from the neutron patterns is shown in the same figure (Fig. 3, left axis). The curve has been built by considering that the S/S_0 value of the local moment at ambient pressure should correspond to the theoretical moment value ($4\mu_B$). As mentioned previously, the ordered moment at ambient pressure is well below the theoretical $4\mu_B$ expected value and decreases upon pressure in the $Pmn2_1$/*Pnma* and block-like phase. In the *Cmcm* phase, the amplitude of the ordered moment is closer to the local moment, suggesting that most of the moment participates in the magnetic ordering. Finally, in the SC region, it is striking that the absence of visible magnetic ordering comes along a finite local magnetic moment. This residual local magnetic moment remains available to produce magnetic fluctuations associated with the neighboring magnetic phase and potential precursor of the SC phase.

Conclusion

Our results evidence a modification of the magnetic order in $BaFe_2Se_3$ as a function of pressure. This modification is likely to be connected to the structural transition toward the *Cmcm* structure as it occurs at the same critical pressure of 3–4 GPa. Under high pressure, $BaFe_2Se_3$ adopts the magnetic order of the parent $BaFe_2S_3$ compound : a magnetic structure characterized by a CX AFM phase with a propagation wave vector $\vec{k} = (\frac{1}{2}, 0, \frac{1}{2})$ and a FM order along the ladder's rung. The regular AFM order between successive Fe–Fe pairs along the ladder's legs indicated that the J_1 and J_1' exchange couplings become similar, where J_1 and J_1' are the two exchange interactions between the nearest-neighbor Fe atoms along the legs (Fig. 1d). This is not surprising because the *Cmcm* symmetry above 3–4 GPa imposes identical Fe–Fe bonds and Se–Fe–Se angles along the legs of the ladder, and thus strictly identical J_1 and J_1'. On the contrary, the $Pmn2_1$ symmetry of the structure at ambient pressure leads to different bounds' lengths and Se–Fe–Se angles and a variety of exchange couplings at the origin of the complex block-like magnetic order.

This CX magnetic order in $BaFe_2Se_3$ is the ground state in a large pressure range from 3 to 4 GPa to at least 7.7 GPa. While no evidence of such a phase in the SC phase (11.7 GPa) could be proven, it is difficult to exclude it completely because of the reduced sensitivity inherent to high-pressure experiments. Our results are supported by DFT calculations[28], predicting such order at high pressure. Despite a disagreement between measured and predicted critical pressure, this theoretical result attests to the proximity in energy of the CX magnetic phase to the point of becoming the ground state with sufficient pressure. Most interestingly, for the parent compound $BaFe_2S_3$, the very same CX magnetic order is the ground state at ambient pressure and persists until 10 GPa[8], a pressure at which the superconductivity emerges. $BaFe_2X_3$ compounds with X = S,Se are expected to present a very similar superconducting mechanism as their crystallographic and magnetic structures are quasi-identical close to the SC phase. In addition, an iso-electronic substitution at the Se site acts as a chemical pressure and should not strongly affect the mechanisms of stabilization of the various ground states within the phase diagram. The stabilization of the universal CX phase in pressurized Fe spin ladders is of great interest due to its closeness to the SC dome. We indeed showed here that the magnetic and SC phases are surely <2 GPa apart. Taking into account the state of the art from cuprates and in the current context of the discovery of superconductivity in U-based ferromagnetic materials such as UGe_2[34] and UCoGe[35], one can foresee the importance of this phase's magnetic fluctuations in the SC mechanism of Fe spin ladders. In the $BaFe_2Se_3$ spin ladder, the presence of magnetic fluctuations is supported by the sudden drop of magnetic order combined with a non-zero local moment in the SC dome. Finally, we show here that these magnetic fluctuations, that are related to the universal stripe-like order at $\vec{k}$ =(1/2, 0, 1/2) are very involved in the SC mechanism in these spin ladders $BaFe_2X_3$ (X = S, Se). $\vec{k} = (\frac{1}{2}, 0, \frac{1}{2})$. Our experimental work will certainly open the way to new theories of Cooper pairing in the iron-based superconductors, simplified by the low dimensionality of the ladder geometry.

Methods

Synthesis. $BaFe_2Se_3$ single crystals were grown using a melt-growth method[14]. Small pieces of Ba (99.9%), powder of Fe (99.9%), and Se (99.999%) were weighed, and mixed with the nominal composition 123. The mixture is placed in a carbon crucible and then sealed in an evacuated quartz tube with a pressure of 300 mbar of Ar gas. The sample was heated at 1150 °C and melted for 24 h. The temperature was afterward lowered to 750 °C at a rate of 5 °C/h, then the furnace was cooled down to room temperature at 100 °C/h. A big polycrystal with a diameter of 10 mm was obtained. Then, the crystal was ground to powder for the diffraction measurements.

X-ray diffraction under pressure. The X-ray diffraction patterns of $BaFe_2Se_3$ at room temperature were collected on the high-pressure diffraction setup developed at LPS. The X-ray source was a Rigaku Mo rotating anode ($\lambda = 0.71$ Å) combined with a 2D MAR345 detector. The Diamond Anvil Cell (DAC) with diamonds of 1 mm diameter was equipped with a CuBe gasket of 70 µm thick. The sample chamber is 500 µm in diameter. The powder was loaded together with a ruby chip and Si oil transmitting medium (hydrostatic up to 10 GPa). The pressure was then measured using the standard ruby fluorescence technique.

Neutron experiment. Temperature dependence of powder neutron diffraction experiments at ambient pressure were carried out on a powder sample with a mass of 1 g, on the G4.1 diffractometer (Orphée-LLB, CEA-Saclay, France). The neutron wavelength was 2.426 Å. For the refinement of the structure, we used the block models proposed in ref. [28].

The powder neutron experiments under pressure were performed on the D1B spectrometer at ILL[36]. We used a Paris–Edinburgh pressure cell with a sample volume of about 50 mm^3, and ethanol-methanol as the pressure-transmitting medium to obtain hydrostatic compression up to 12 GPa. Lead (Pb) was placed inside the anvil cell enabling pressure estimation at all pressures and temperatures using the Pb diffraction pattern combined with its equation of state. The calibration of the experimental parameters (zero, wavelength, *u*, *v*, *w*) was performed at ambient conditions with $Al_2Ca_3F_{14}Na_2$ powder. The pressure in the cell was determined by the lattice parameters of the lead after refinements. We first obtained a_0(Pb) = 4.9398 A° at ambient temperature, indicating a pressure of 0.3 GPa. Then, the pressure was increased, followed by a cooling down to 3 K. Based on a_0(Pb) and the equation of state (EOS) of Pb, we get the pressure according to a_i(Pb) in each measurement[37].

The refinements for both the crystal and magnetic structures were performed by using FULLPROF suite[38].

X-ray emission spectroscopy. To probe the evolution of the local magnetic moment on the Fe site, we performed X-ray emission spectroscopy (XES) at the GALAXIES beamline[39] of Synchrotron SOLEIL. A DAC was used to increase the pressure. $BaFe_2Se_3$ pieces of crystals were loaded in a 150 µm hole of a CuBe gasket, along with ruby chips for in situ pressure measurement and silicone oil as a pressure-transmitting medium. XES were measured with the spectrometer in a transmission geometry using a 1 m radius spherically bent Ge(620) crystal analyzer and an avalanche photodiode detector arranged in the Rowland circle geometry. The total energy resolution at the Fe K_β line (≈7057 eV) was 1.2 eV FWHM. The XES spectra were measured with 10 keV incident energy, above the K edge.

Data availability

The data that support the findings of this study are available from the authors on reasonable request, see author contributions for specific data sets. Besides, the neutron diffraction data under pressure are available at ILL database[36].

Received: 29 November 2021; Accepted: 27 June 2022;
Published online: 14 July 2022

References

1. Hegger, H. et al. Pressure-Induced superconductivity in quasi-2D $CeRhIn_5$. *Phys. Rev. Lett.* **84**, 4986–4989 (2000).
2. Knebel, G. et al. Field-reentrant superconductivity close to a metamagnetic transition in the heavy-fermion superconductor UTe_2. *J. Phys. Soc. Jpn.* **88**, 063707 (2019).
3. Jérome, D., Mazaud, A., Ribault, M. & Bechgaard, K. Superconductivity in a synthetic organic conductor $(TMTSF)_2PF_6$. *J. Phys. Lett.* **41**, 95–98 (1980).
4. Uemura, Y. Energy-scale phenomenology and pairing via resonant spin-charge motion in FeAs, CuO, heavy-fermion and other exotic superconductors. *Phys. B Condens. Matter* **404**, 3195–3201 (2009).
5. Chen, H. et al. Coexistence of the spin-density wave and superconductivity in $Ba_{1-x}K_xFe_2As_2$. *EPL* **85**, 17006 (2009).
6. Sanna, S., Allodi, G., Concas, G., Hillier, A. D. & Renzi, R. D. Nanoscopic coexistence of magnetism and superconductivity in $YBa_2Cu_3O_{6+x}$ detected by muon spin rotation. *Phys. Rev. Lett.* **93**, 207001 (2004).
7. Nickel, J. C., Duprat, R., Bourbonnais, C. & Dupuis, N. Triplet superconducting pairing and density-wave instabilities in organic conductors. *Phys. Rev. Lett.* **95**, 247001 (2005).
8. Takahashi, H. et al. Pressure-induced superconductivity in the iron-based ladder material $BaFe_2S_3$. *Nat. Mater.* **14**, 1008 (2015).
9. Ying, J., Lei, H., Petrovic, C., Xiao, Y. & Struzhkin, V. V. Interplay of magnetism and superconductivity in the compressed Fe-ladder compound $BaFe_2S_3$. *Phys. Rev. B* **95**, 241109 (2017).
10. Hong, H. & Steinfink, H. The crystal chemistry of phases in the Ba–Fe–S and Se systems. *J. Solid State Chem.* **5**, 93–104 (1972).
11. Zheng, W. et al. Room temperature polar structure and multiferroicity in $BaFe_2Se_3$. *Phys. Rev. B* **101**, 020101 (2020).
12. Dong, S., Liu, J. M. & Dagotto, E. $BaFe_2Se_3$: a high T_C magnetic multiferroic with large ferrielectric polarization. *Phys. Rev. Lett.* **113**, 187204 (2014).
13. Caron, J. M., Neilson, J. R., Miller, D. C., Llobet, A. & McQueen, T. M. Iron displacements and magnetoelastic coupling in the antiferromagnetic spin-ladder compound $BaFe_2Se_3$. *Phys. Rev. B* **84**, 180409 (2011).
14. Lei, H., Ryu, H., Frenkel, A. I. & Petrovic, C. Anisotropy in $BaFe_2Se_3$ single crystals with double chains of FeSe tetrahedra. *Phys. Rev. B* **84**, 214511 (2011).
15. Nambu, Y. et al. Block magnetism coupled with local distortion in the iron-based spin-ladder compound $BaFe_2Se_3$. *Phys. Rev. B* **85**, 064413 (2012).
16. Gao, J. et al. The synthesis and magnetic properties of $BaFe_2S_3$ single crystals. *RSC Adv.* **7**, 30433–30438 (2017).
17. Mourigal, M. et al. Block magnetic excitations in the orbitally selective Mott insulator $BaFe_2Se_3$. *Phys. Rev. Lett.* **115**, 047401 (2015).
18. Saparov, B. et al. Spin glass and semiconducting behavior in one-dimensional $BaFe_2Se_3$ crystals. *Phys. Rev. B* **84**, 245132 (2011).
19. Svitlyk, V. et al. Crystal structure of $BaFe_2Se_3$ as a function of temperature and pressure: phase transition phenomena and high-order expansion of Landau potential. *J. Phys. Condens. Matter* **25**, 315403 (2013).
20. Sun, H. et al. Nonsuperconducting electronic ground state in pressurized $BaFe_2S_3$ and $BaFe_2S_2.5Se0.5$. *Phys. Rev. B* **101**, 205129 (2020).
21. Krzton-Maziopa, A. et al. The synthesis, and crystal and magnetic structure of the iron selenide $BaFe_2Se_3$ with possible superconductivity at $t_c = 11$ K. *J. Phys. Condens. Matter* **23**, 402201 (2011).
22. Liu, X. et al. Structural, magnetic and dielectric properties of $BaFe_2S_3$ crystals. *EPL* **126**, 27005 (2019).
23. Medvedev, M. V., Nekrasov, I. A. & Sadovskii, M. V. Electronic and magnetic structure of a possible iron based superconductor $BaFe_2Se_3$. *JETP Lett.* **95**, 33–37 (2012).
24. Rincon, J., Moreo, A., Alvarez, G. & Dagotto, E. Exotic magnetic order in the orbital-selective Mott regime of multiorbital systems. *Phys. Rev. Lett.* **112**, 106405 (2014).
25. Lovesey, S. W., Khalyavin, D. D. & van der Laan, G. Neutron diffraction and the electronic properties of $BaFe_2S_3$. *Phys. Scr.* **91**, 015803 (2016).
26. Herbrych, J. et al. Spin dynamics of the block orbital-selective Mott phase. *Nat. Commun.* **9**, 3736 (2018).
27. Svitlyk, V. et al. High-pressure polymorphism of $BaFe_2S_3$. *J. Phys. Condens. Matter* **31**, 085401 (2019).
28. Zhang, Y., Lin, L.-F., Zhang, J.-J., Dagotto, E. & Dong, S. Sequential structural and antiferromagnetic transitions in $BaFe_2S_3$ under pressure. *Phys. Rev. B* **97**, 045119 (2018).
29. Wu, S. et al. Robust block magnetism in the spin ladder compound $BaFe_2Se_3$ under hydrostatic pressure. *Phys. Rev. B* **100**, 214511 (2019).
30. Caron, J. M. et al. Orbital-selective magnetism in the spin-ladder iron selenides $Ba_{1-x}K_xFe_2Se_3$. *Phys. Rev. B* **85**, (2012).
31. Materne, P. et al. Bandwidth controlled insulator–metal transition in bafe 2 s 3: a Mössbauer study under pressure. *Phys. Rev. B* **99**, 020505 (2019).
32. Rueff, J.-P. et al. Pressure-induced high-spin to low-spin transition in fes evidenced by x-ray emission spectroscopy. *Phys. Rev. Lett.* **82**, 3284–3287 (1999).
33. Norman, M. R. Colloquium: Herbertsmithite and the search for the quantum spin liquid. *Rev. Mod. Phys.* **88**, 041002 (2016).
34. Saxena, S. S. et al. Superconductivity on the border of itinerant-electron ferromagnetism in UGe_2. *Nature* **406**, 592 (2000).
35. Aoki, D., Ishida, K. & Flouquet, J. Review of U-based ferromagnetic superconductors: comparison between UGe_2, URhGe, and UCoGe. *J. Phys. Soc. Jpn.* **88**, 022001 (2019).
36. Zheng, W. G., Balédent, V., Colin, C. V. & Foury-Leylekian, P. *Experimental Data: Study of the Competition Between Magnetism and Superconductivity in $BaFe_2Se_3$*. https://doi.org/10.5291/ILL-DATA.CRG-2770 (2021), https://doi.org/10.5291/ILL-DATA.5-31-2722 (2020), https://doi.org/10.5291/ILL-DATA.5-31-2639 (Institut Laue-Langevin (ILL), 2019).
37. Strässle, T., Klotz, S., Kunc, K., Pomjakushin, V. & White, J. Equation of state of lead from high-pressure neutron diffraction up to 8.9 GPa and its implication for the NaCl pressure scale. *Phys. Rev. B* **90**, 014101 (2014).
38. Rodríguez-Carvajal, J. Recent advances in magnetic structure determination by neutron powder diffraction. *Phys. B Condens. Matter* **192**, 55–69 (1993).
39. Rueff, J.-P. et al. The GALAXIES beamline at the SOLEIL synchrotron: inelastic X-ray scattering and photoelectron spectroscopy in the hard X-ray range. *J. Synchrotron Radiat.* **22**, 175–179 (2015).

Acknowledgements

We acknowledge M.B. Lepetit and M. Mostovoy for very fruitful discussions. We also thank SOLEIL for synchrotron beam time (Proposal 20200410) as well as Claude Payre, James Maurice, Sofien Djellit, Vivian Nassif, and Ines PUENTE ORENCH for the D1B experiment. Experiments at ILL were sponsored by the French Neutron Federation (2FDN). This work was financially supported by the ANR COCOM 20-CE30-0029 and supported by the CSC scholarship (No. 201806830111).

Author contributions

W.-G.Z., P.F.-L, V.B., C.V.C., J.-P.R. and F.D. performed the various experiments. W.-G.Z., V.B., P.F.-L. analyzed the data. D.C. and A.F. synthesized the sample.

Competing interests

The authors declare no competing interests.

Additional information

Supplementary information The online version contains supplementary material available at https://doi.org/10.1038/s42005-022-00955-7.

Correspondence and requests for materials should be addressed to Pascale Foury-Leylekian.

Peer review information *Communications Physics* thanks Shan Wu and the other, anonymous, reviewer(s) for their contribution to the peer review of this work.

Reprints and permission information is available at http://www.nature.com/reprints

Publisher's note Springer Nature remains neutral with regard to jurisdictional claims in published maps and institutional affiliations.